Physics Letters B 795 (2019) 554–560

Contents lists available at ScienceDirect

Physics Letters B

www.elsevier.com/locate/physletb

Significant improvement of half-life calculation of α decays by considering the nuclear medium effect

Daming Deng [a,c], Zhongzhou Ren [b,c,*], Nan Wang [a,**]

[a] College of Physics, Shenzhen University, Shenzhen 518060, China
[b] School of Physics Science and Engineering, Tongji University, Shanghai 200092, China
[c] Department of Physics, Nanjing University, Nanjing 210093, China

ARTICLE INFO

Article history:
Received 6 January 2019
Received in revised form 25 April 2019
Accepted 21 June 2019
Available online 4 July 2019
Editor: J.-P. Blaizot

Keywords:
α decay
Half-life
Nuclear medium effect
α clustering
α-preformation factor

ABSTRACT

We incorporate the nuclear medium effect into α-decay calculation through a reformulation of the conventional double-folding model. The improved model enables the α cluster to simultaneously change its size at different nuclear density during the Coulomb penetration process, thus reflecting the effect from the variation of nuclear mean field and Pauli blocking at the nuclear surface. To evaluate the result of such a dynamic effect, we perform a systematic calculation of α-decay half-lives for even-even α-emitters within a deformed cluster model. We found that the medium effect optimises the shape of α-nucleus potential at the surface region, leading to a remarkable reduction in the deviations between the theoretical and experimental decay rates. The result implies the importance of the dynamic aspect of α clustering in describing a realistic α-nucleus interaction.

1. Introduction

The mechanism of clustering in nuclei is an important subject in nuclear many-body physics. The single-particle characteristics of nuclear motion are described by the well-known shell model, in which the shell structure appears as a manifestation of the mean-field effect. On the other hand, the vibrational and rotational bands observed from experimental excitation spectrums can be well explained within the collective model. The collective model serves as an important supplement to the shell-model description, reflecting the global properties of a nucleus from a different perspective [1]. Compared with the two types of dynamics above, clustering characterizes another type of motion, seemingly as an in-between mode of the single-particle and the collective motions, which describes the competition of correlation dynamics within local nucleons especially when one typical correlation becomes prominent. Research on the cluster states in light nuclei has revealed that clustering leads to new degrees of freedom for nuclear motions, the relative motion and the intrinsic motion of clusters, which are essential to the interpretation for some unique excitation spectrums observed from experiments [2]. With clustering in light nuclei being well confirmed and studied, to explore the cluster structures in heavy nuclei is becoming increasingly important.

Unlike the situation for light nuclei, the knowledge of clustering phenomenon in heavy nuclei is very limited [3]. On one hand, there are very few experimental observations for the cluster states in heavy nuclei. In fact, even the most promising cluster states, i.e. the core + α states, are only observed or predicted for some special nuclei, such as ^{212}Po which can be viewed as a double-magic core plus an α cluster [4–8]. On the other hand, theoretical description of clustering in heavy nuclei poses a big challenge to the existing nuclear models. It is already confirmed that traditional shell-model calculations cannot produce sufficient α-clustering at the nuclear surface [9], and microscopic cluster models that work well for light nuclei, have encountered substantial difficulties for heavy nuclei while dealing with the antisymmetrized effects [10]. The physical connection between clustering in light nuclei and heavy nuclei is still ambiguous, which calls for new methods and models to understand the mechanism of clustering in heavy systems.

Alpha decay is a direct clue to the existence of α clustering in heavy nuclei. As one of primary decay modes of unstable nuclei, α decay has been well understood as a kind of quantum tunneling effect. Within the basic assumption of cluster models, there is a probability that the α cluster is preformed inside the

* Corresponding author at: School of Physics Science and Engineering, Tongji University, Shanghai 200092, China.
** Corresponding author.
E-mail addresses: ddm@szu.edu.cn (D. Deng), zren@tongji.edu.cn (Z. Ren), wangnan@szu.edu.cn (N. Wang).

https://doi.org/10.1016/j.physletb.2019.06.045

parent nucleus. Such probability is usually described by the so-called α-preformation factor (P_α), a quantity determined by the square overlap between the α-nucleus decaying state and the initial wavefunction of the α emitter. Obviously, the P_α factor is closely related to the α-cluster states in heavy nuclei because its magnitude directly reflects the amount of α clustering in the initial state of the α emitter. Therefore, studies of the α-preformation factor provides a path to investigate the cluster structure as well as other structural properties in heavy nuclei.

In general, to characterize the clustering phenomenon in heavy nuclei from a microscopical level is very difficult. To obtain adequate clustering features for the initial state at the nuclear surface, within a shell-model approach, one has to employ a very large-scale bases and include the contribution from high-lying configurations [11–14]. The calculation is so complicated and thus only valid for nuclei around shell closures. A combination of shell-model and cluster-model bases can simplify the calculation to some extent [4], but such a hybrid model is inherently designed for those "core + α" nuclei. So it is difficult to generalize to nuclides with more valence nucleons included. To describe the α formation process in heavy nuclei, researchers also attempt to extend the α-clustering studies from nuclear matter to finite nuclei. Recently, the quartetting wavefunction approach based on such attempt was successfully applied to ^{212}Po and its nearby isotopes [15–17]. Treating the four nucleons (α) in a fully quantum-mechanical formulism, the formation of the α cluster was described as a transition from shell-model continuum states to a bound intrinsic cluster state, with an effective potential for the center-of-mass motion derived. Despite the approach has assumed the daughter nucleus as a kind of nuclear medium to the four nucleons (α), the microscopic calculation reveals more details inside the α emission process. As one distinct feature, the α cluster is found to dynamically changes its size while tunnelling the Coulomb potential barrier. Such dynamics during the decay process can be viewed as a kind of nuclear medium effect, which emerges with the variation of the nuclear mean field and Pauli blocking at the nuclear surface.

Obviously, the nuclear medium effect should also appear in the α-nucleus potential. The size variation of the α cluster implies the change of its density distribution and nucleon-nucleon interactions, which is not considered in previous cluster-model calculations. As for α decay, it is known that the calculation of decay half-lives and α-preformation factors is very sensitive to the adopted α-nucleus potential, especially the surface region where the nuclear medium effect is just evident. In a previous research, we attempted to incorporate this nuclear medium effect into the α-nucleus potential within the microscopic double-folding model [18]. Alternative to the quartetting wavefunction approach, the medium effect directly enters into the α-nucleus potential through a dynamical density distribution of the α cluster. Exploratory calculations were performed for even-even spherical nuclei to evaluate its influence. With some positive results obtained, the conclusion reached is yet limited due to the absence of the nuclear deformation. In order to obtain a comprehensive view of the nuclear medium effect in α decay, the calculation should be carried out in wide range of the nuclide chart, for which the nuclear deformation has to be properly considered.

In this letter, we report the systematic study of the nuclear medium effect in α decay from the perspective of decay half-life, α-preformation factor (P_α) and most importantly, the α-nucleus potential. The dynamic double-folding potential (DDFP) for deformed α-nucleus interactions is developed, which embodies the dynamic effect that the α cluster varies its size at different baryon density throughout the nuclear surface. The computation of deformed DDFP is extremely time consuming (about 1000 times more than the spherical case), but the improvement to the half-life

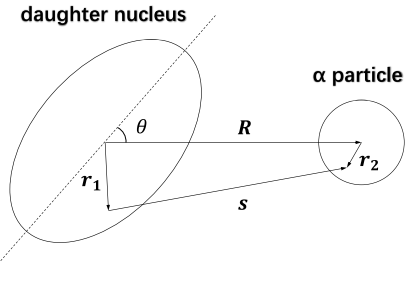

Fig. 1. Schematic illustration of the deformed double-folding potential described by Eq. (1).

calculation is found to be very significant. The results clearly address the importance of the dynamic effect of the α cluster during the decay process. In the next section, starting from the conventional double-folding potential, we provide the theoretical derivation of the deformed DDFP. The method to embed the medium effect into the α-nucleus potential will be explained in details. In Section 3, we demonstrate the numerical results obtained with the DDFP, along with discussions based on comparisons with the conventional calculations. Section 4 is a brief summary and outlook for the present study.

2. Theoretical description

In theories of α decay and α scattering, the α-nucleus interaction is an essential ingredient which reflects the basic characteristics of a theoretical model. In general, this α-nucleus potential can be generated through either a phenomenological or a microscopic procedure. The double-folding potential is a typical representative of the latter [19], which is based on realistic nucleon-nucleon (NN) interactions and the density distributions of the two-body interactive nuclei. For an α-nucleus system where the daughter nucleus is of axial symmetry (Fig. 1), the deformed double-folding potential is given by [20],

$$V_{N(C)}(R,\theta) = \lambda \int d\mathbf{r_1} d\mathbf{r_2} \rho_1(\mathbf{r_1}) \rho_2(r_2) \upsilon_{N(C)}(\mathbf{s}), \tag{1}$$

where $\rho_1(\mathbf{r_1})$ and $\rho_2(r_2)$ are the charge or matter density distributions of the daughter and α clusters, and the corresponding NN interactions for the nuclear and Coulomb potentials are denoted by $\upsilon_{N(C)}(\mathbf{s})$. Usually, an additional parameter λ has to be introduced to renormalize the strength of $\upsilon_N(\mathbf{s})$ ($\lambda \equiv 1$ for the Coulomb potential).

For clustering phenomena in heavy nuclei, α cluster tends to appear at the nuclear surface of low nuclear density [13,15,21–25]. After the formation of the α cluster, the effective interaction felt by the α cluster is mainly determined by the nuclear mean field produced by the residual nucleons and the Pauli blocking effect appearing at the nuclear surface. Since Pauli blocking suppresses the four-nucleon (α) occupations at the Fermi level, the NN interactions within the α cluster would change accordingly at different nuclear density. As a result, the intrinsic α-cluster wavefunction changes simultaneously as the cluster is moving outside the nuclear surface. To exactly determine the dynamics of the α cluster at different nuclear density, one has to solve the in-medium Schrodinger equation for the intrinsic motion of the α cluster. This was done in Ref. [15] with the recently proposed quartetting wavefunction approach. By employing a fully quantal treatment for the four-nucleon (α) cluster in homogeneous nuclear matter, the authors successfully determined the intrinsic energy shift due to the Pauli blocking as a function of baryon density. Within a variational

approach, the quartetting wavefunction for the α cluster was determined in local density approximation (LDA). It was found that due to the medium effect, the α cluster expands its density distribution in finite density, which corresponds to a larger radius than that of a free α particle. On the other hand, as the nuclear density decreases at the nuclear surface, the variation of Pauli blocking will result in a dynamical transformation of the α-cluster density distribution, meaning that the α cluster will dynamically change its size while penetrating the Coulomb potential barrier.

Backing to the formulation of Eq. (1), one can recognize that both the density distributions of the daughter and α clusters are taken to be frozen. This implies that while calculating the double-folding α-nucleus potential, the nuclear medium effect discussed above is not explicitly considered. As is known, the calculation of α-decay rates is very sensitive to the α-nucleus potential, especially its surface geometry between the inner and outer classical turning points. This is exactly the range where the nuclear medium effect is evident according to previous microscopic calculations [15, 16]. Hence, for a more realistic behavior of the α-nucleus potential, the dynamics of the α cluster during its emission has to be properly considered into the α-nucleus interaction.

In such attempt, we propose the dynamical double-folding potential (DDFP) which is of the general form,

$$V_C(R,\theta) = \int d\mathbf{r_1} d\mathbf{r_2} \rho_1(\mathbf{r_1}) \rho_2(r_2, \rho_1(\mathbf{R})) \upsilon_C(\mathbf{s}), \tag{2}$$

$$V_N(R,\theta) = \lambda \int d\mathbf{r_1} d\mathbf{r_2} \rho_1(\mathbf{r_1}) \rho_2(r_2, \rho_1(\mathbf{R})) t(\mathbf{s}, \rho_1, \rho_2, E_\alpha), \tag{3}$$

with $\mathbf{R} \equiv \{R, \theta\}$ in the above equations. To incorporate the nuclear medium effect, a simple idea is that the α-cluster density distribution should be treated dynamically, i.e., dependent on the density n_B of the surrounding nuclear medium in LDA. Therefore, the $\rho_2(r_2)$ in Eq. (1) can be rewritten into $\rho_2(r_2, n_B)$. For an α-daughter system, the medium density is given by the density distribution of daughter nucleus, such that we have $\rho_2(r_2, \rho_1(\mathbf{R}))$ as in Eq. (3). In addition, with the α-cluster density distribution taken dynamically, one might also consider that the daughter's density-distribution as well as the NN interaction should also change self-consistently from a many-body viewpoint. For the nuclear part of NN interactions, this can be achieved by replacing $\upsilon_{(N)}(\mathbf{s})$ in Eq. (1) with a density-dependent NN interaction. In the present study, the CDM3Y6 parameterized NN interaction $t(\mathbf{s}, \rho_1, \rho_2, E_\alpha)$ is employed [26], in which the density dependence is characterized by

$$f(\rho_1, \rho_2) = C_1[1 + C_2 e^{-C_3(\rho_1+\rho_2)} - C_4(\rho_1 + \rho_2)], \tag{4}$$

where $C_{i=1,2,3,4}$ are parameters determined through reproducing the saturation properties of normal nuclear matter within Hartree-Fock calculations in [26].

To consider the dynamics of the daughter's density distribution means the dependence of the internuclear position $\mathbf{R}$ has to be introduced, which yields $\rho_1(r_1, \mathbf{R})$. However, the determination of the dynamic features of $\rho_1(r_1, \mathbf{R})$ is an extremely complicated problem which so far has not been well studied. Physically, because nucleons of the daughter nucleus are usually much more than of the α cluster, the variation of $\rho_1(r_1)$ resulting from the change of the α-cluster density distribution is expected to be minor. Even in the many-body calculations of Ref. [15], a fixed density distribution for the daughter nucleus was accepted as a basic approximation. Hence, currently in Eq. (3) the frozen density distribution for the daughter nucleus can be retained.

The density-dependence of the α-cluster density distribution is a central problem for the representation of the nuclear medium effect. In calculations of the conventional double-folding α-nucleus potential, $\rho_2(r_2)$ usually takes the typical Gaussian-type as $\rho_2(r_2) = \rho_{2,s} \exp(-\beta r_2^2)$, with the width parameter $\beta = 0.7024$ determined by reproducing the charge r.m.s radius 1.67 fm from experiments. Being aware of that this width parameter controls the size of the α cluster, we thus can embed the density-dependence into β such that the density distribution ρ_2 becomes

$$\rho_2(r_2, \rho_1(\mathbf{R})) = \rho_{2,s} \exp[-\beta(\rho_1(\mathbf{R}))r_2^2]. \tag{5}$$

In this way, the α cluster can simultaneously change its size at different baryon density through the variation of β. In order to determine the density-dependence of β, in our previous study [18], we extracted the dynamic features of the α cluster from the existing research and transformed into mathematical constrains of $\beta(n_B)$. Through a couple of trails, we found the nuclear medium effect can be well described with a simple formula,

$$\beta(n_B) = \frac{0.7024}{1 + a_1 n_B}. \tag{6}$$

Here, the only parameter a_1 is not adjustable, but determined by the saturation density $\rho_{1,s}$ of the daughter nucleus, with $a_1 = \frac{45}{16\rho_{1,s}}$. While calculating the DDFP, both $\rho_{1,s}$ and $\rho_{2,s}$ are determined by normalization of the density distributions to the charge or mass number of the corresponding nuclei.

The medium effect described by Eqs. (6) is demonstrated in Fig. 2. One can find the variation of β automatically changes the size of the in-medium α cluster (characterized by peak density $\rho_{2,s}$ and root-mean-square charge radius R_{rms}) at different medium density. Moreover, a qualified $\beta(n_B)$ function should be able to reproduce the critical characteristics suggested by both microscopic calculations and experiments. For instance, at zero density limits, β automatically goes to the typical value 0.7024 fm^{-2} corresponding to the experimental charge r.m.s radius of a free α particle (1.67 fm). Additionally, $\beta(\rho_1(\mathbf{R}))$ smoothly decreases at smaller internuclear distance, reflecting that at the nuclear surface, the α cluster gradually reduces its size while moving outside the Coulomb potential barrier. In particular, the values reached by the square root of β at one-fifth the saturation density is 20% smaller than that at the zero density limit, consistent with the result of Refs. [15, 18]. These quantitative relations are used to determine the coefficient a_1 in Eq. (6) [18]. Besides, while approaching the region of higher density into the daughter nucleus, the distribution ρ_2 becomes flattened so that can simulate the shell-model continuum

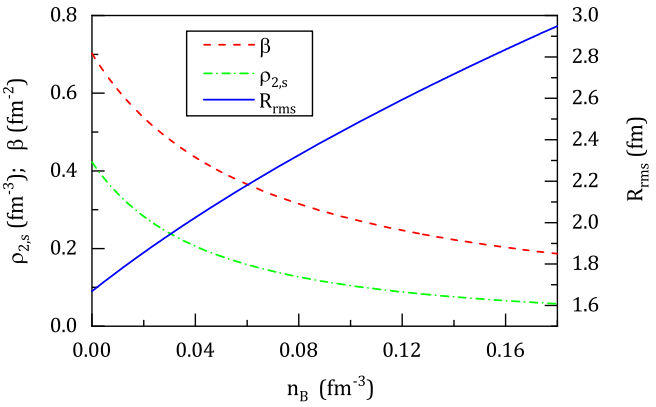

Fig. 2. The medium effect on the α cluster described by Eqs. (6). The green dot-dashed line and the blue solid line represent the peak density $\rho_{2,s}$ of the α-cluster density distribution and the corresponding root-mean-square charge radius R_{rms}. The width parameter β (red dashed line) slowly decreases with higher medium density n_B, implying that the in-medium α cluster will smoothly increase its size while moving closer to the daughter nucleus.

states at the internal region. In short, the nuclear medium effect is embedded through the width parameter β of the α-cluster density distribution. Once the $\beta(n_B)$ function is determined, the deformed DDFP potential can be calculated according to Eqs. (2) and (3).

3. Results and discussions

In order to evaluate the influence due to the nuclear medium effect in α decay, we perform a systematic calculation of the α-decay half-lives among the known even-even α emitters. A total of 180 nuclei with $106 \leqslant A \leqslant 294$ are studied, in which 135 nuclei are well-deformed. Most of these nuclei go through the favored α decays, with almost 100% intensity for the 0^+ to 0^+ ground-state transition. Hence, it would be favorable for us to observe the pure manifestation of the nuclear medium effect, because additional factors such as the angular momentum transferred to the α particle and the change of spin-parity between the initial and the final states can be excluded.

Besides, it should be noted that the consideration of nuclear deformation of the daughter nucleus is very important because the medium effect under study is strongly dependent on the density distribution $\rho_1(\mathbf{r_1})$. However, the combined consideration of deformation and the medium effect along with a density-dependent NN interaction will considerably increase the computational intense. For the daughter nucleus of axial-symmetrical deformation, $\rho_1(\mathbf{r_1})$ can be described by the two-parameter Fermi function $\rho_1(r_1,\theta) = \rho_{1,s}/(1+\exp[(r_1-\tilde{R}(\theta))/\tilde{a}])$ [18,20]. The half-density radius $\tilde{R}(\theta) = R_0[1+\beta_2 Y_{20}(\theta)+\beta_4 Y_{40}(\theta)]$ is associated with the quadrupole and hexadecapole deformation parameters β_2 and β_4, and introduces the dependence on orientation θ. To obtain the deformed DDFP, one has to calculate numerically the Fourier transformation of the term $\rho_2(r_2,R,\theta)\exp[-C_3\rho_2(r_2,R,\theta)]$ at the full (R,θ) space. Combined with the multipole expansion of the deformed potential and the daughter's density distribution, the time consumption for one nucleus is about one thousand times more than of the spherical case within the same calculation precision. This is a basic requirement before making any direct comparisons between the DDFP and the conventional double-folding potential. With both potentials determined, the penetrability P for a certain orientation θ can be evaluated through the well-known Wentzel-Kramers-Brillouin (WKB) approximation,

$$P(\theta) = \exp(-2\int_{R_2(\theta)}^{R_3(\theta)} \sqrt{\frac{2\mu}{\hbar^2}|V(R,\theta)-Q_\alpha|}dR). \tag{7}$$

Then the total penetrability is obtained by averaging $P(\theta)$ in all directions [20],

$$P = \frac{1}{2}\int_0^\pi P(\theta)\sin(\theta)d\theta. \tag{8}$$

Finally, the half-life is given by [18,20,27]

$$T_{1/2} = \frac{\ln 2}{P_\alpha F \frac{\hbar}{4\mu} P}. \tag{9}$$

In Fig. 3 the deviations of α-decay half-lives calculated by using the conventional double-folding potential and the DDFP are presented. Within the present half-life calculation, one should employ the P_α factor as a theoretical input. Since the P_α factor for a certain type (even-even/odd-A/odd-odd) of nuclei only varies slightly in the open-shell region [28,29], we adopt a constant P_α factor

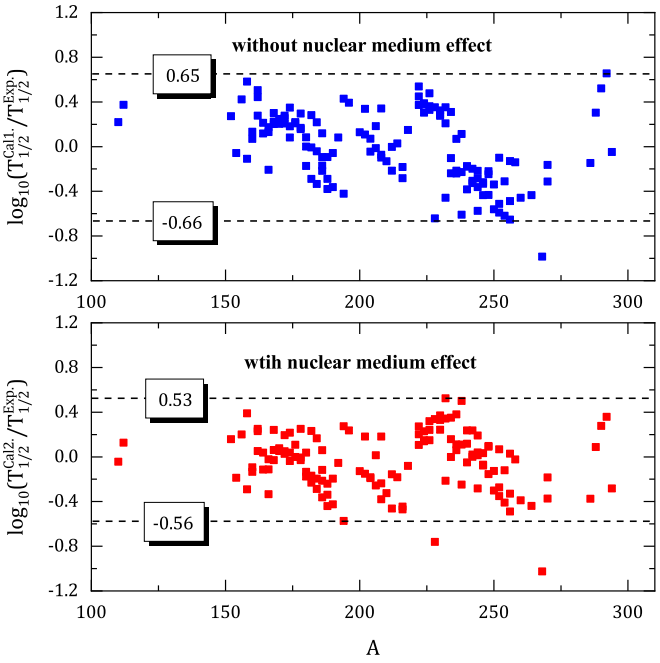

Fig. 3. Deviation between the calculated α-decay half-life and the corresponding experimental value. $T^{Cal1.}_{1/2}$ and $T^{Cal2.}_{1/2}$ denote the theoretical α-decay half-lives calculated with the conventional double-folding potential (without the nuclear medium effect) and the DDFP (with the nuclear medium effect), respectively. The inclusion of the nuclear medium effect significantly reduces the average deviation by about 23%.

which is determined through a least square fitting of the half-life deviation. Moreover, the calculation is only conducted for the 135 well deformed nuclei which are located far from the neutron or proton shell closure. In this way, one can ensure the obtained half-life deviations are mainly due to the differences in the α-nucleus potential.

As can be observed from Fig. 3, after the nuclear medium effect is included into the α-nucleus potential, the deviation between the theoretical and the experimental α-decay half-lives reduces significantly. To evaluate the improvement for the calculated decay rates, one can employ the scale factor $S = 10^\sigma$, with the average deviation factor σ obtained by $\sigma = \frac{1}{N}\sum_{i=1}^{N}|\log_{10}T^{Cal.}_{1/2,i} - \log_{10}T^{Exp.}_{1/2,i}|$. In our calculation, the S factor given by the conventional double-folding potential is 1.88, which means that the theoretical half-lives are statistically within the range 47% smaller to 88% larger than the experimental values. As is known to α-decay calculations, this is already a very good agreement in practice. However, after the nuclear medium effect is included into the α-nucleus potential, the DDFP yields a factor $S = 1.62$, with the average deviation σ further reduced by up to 23%, which is a very significant improvement for half-life calculations. More interestingly, it is found that such reduced deviation is not a monotonic improvement. For example, the calculated half-life of ^{250}Cf increases from 6.00 y to 9.79 y, whereas that of ^{222}Th decreases from 5.29 ms to 2.87 ms. In both cases the theoretical half-lives are getting closer to their experimental values ($T^{Exp.}_{1/2}(^{250}\mathrm{Cf})$ = 13.08 y, $T^{Exp.}_{1/2}(^{222}\mathrm{Th})$ = 2.24 ms) but from opposite directions. The good agreement achieved by the DDFP strongly confirms the importance of the nuclear medium effect in describing a realistic α-nucleus interaction.

Encouraged by the above results, we extract the empirical α-preformation factors from experimental decay rates by using both potentials. In previous calculations for the spherical α emitters near the shell closures [18], it was found that the nuclear medium effect generally reduces the magnitude of the P_α factor,

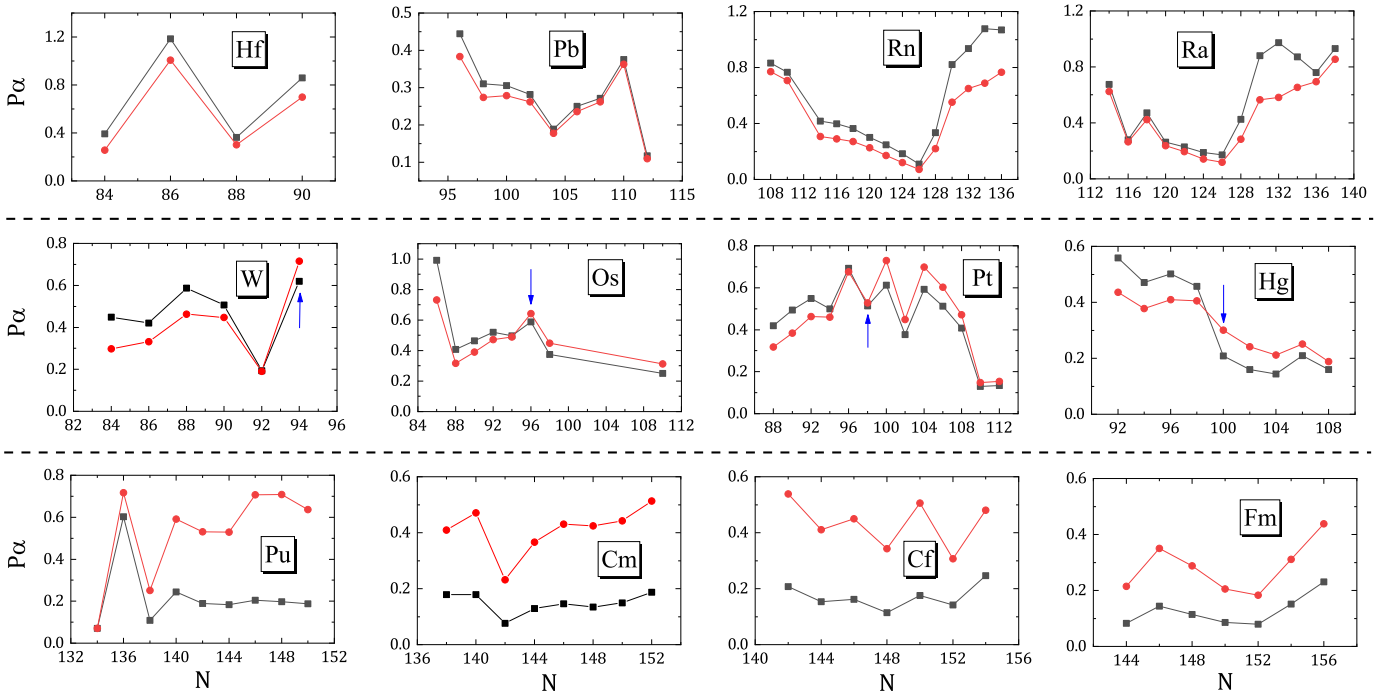

Fig. 4. The variation of α-preformation factors along different isotopic chains. P_α obtained by the DDFP and the conventional double-folding potential are denoted by the red and dark lines, respectively. The results are divided into three categories (rows) according to different manifestations of the nuclear medium effect. The crossovers between P_α variations in the second-row subfigures are marked by the blue arrows.

whereas the trend of the P_α variation with the nucleon number is maintained. In the present study, such calculations are extended to mid-shell nuclei whose deformation cannot be ignored, so there probably exist different manifestations of the nuclear medium effect on α-preformation factors. Fig. 4 shows the variation of P_α factors along different isotopic chains. It is found that the medium effect does not significantly change the trend of P_α factors. But according to different manifestations of the nuclear medium effect, the results can seemingly be divided into three categories (see the separated three rows of the subfigures in Fig. 4). After including the nuclear medium effect, the P_α factors can be either smaller (the first row) or larger (the third row) than before. However, while looking into the P_α variation of W, Os, Pt, Hg isotopes (the second row), one can find that as the neutron number increases, there are crossovers between the results of the two potentials, which seems to imply a transition of the nuclear medium effect between the above two cases.

One probable reason for such transition to appear is the variation of nuclear deformation. This variation changes the surface behavior of the density distribution of the daughter nucleus and thus the α-nucleus potential. It is well known that the penetration probability is extremely sensitive to the α-nucleus potential, especially at the nuclear surface where the nuclear medium effect is important. Therefore, the penetration probability could be enhanced or suppressed by the nuclear medium effect through the variation of the daughter's deformation. In order to illustrate its underlying correlations, we plot in Fig. 5 the ratio of penetrabilities obtained by the two potentials as a function of the quadrupole and hexadecapole deformation parameters of the daughter nucleus. Note that the color map shows the value of $\xi = \log_{10}(P^{med}/P^{no})$ which reflects the change of penetration probability at different deformation parameters. As can be observed from Fig. 5, near the center of the parameter space, ξ is a positive value which means that for spherical and less deformed nuclei, the included medium effect will increase the tunnelling probability of the alpha cluster. In consequence, the extracted P_α factor decreases accordingly, which exactly agrees with the results from previous study [18]. When moving away from the center, ξ gradually reduces and becomes a negative value towards the up-right corner of the parameter space. Such behavior certainly indicates that there would be a transition for the variation of penetrability (so does P_α) when ξ changes its sign. If one refers to the deformation parameters of the isotopes studied in Fig. 4, it becomes easy to understand the existence of three types of behaviors for the P_α variation.

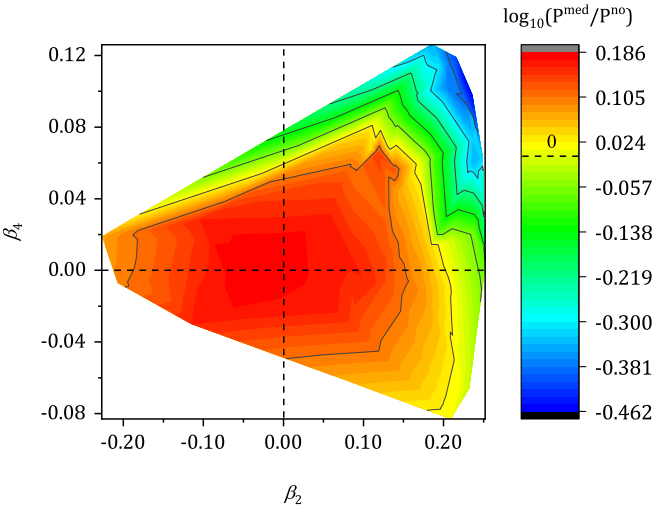

Fig. 5. The ratio of penetration probabilities as a function of deformation parameters of the daughter nucleus. P^{med} and P^{no} denote the penetrability obtained by the DDFP and the conventional double-folding potential, respectively.

Besides the different behaviors mentioned above, another striking feature of Fig. 4 is that the magnitude of P_α for isotopes $Z \geq 94$ are obviously larger after the medium effect is included. This implies there exists an obvious variation in the geometry

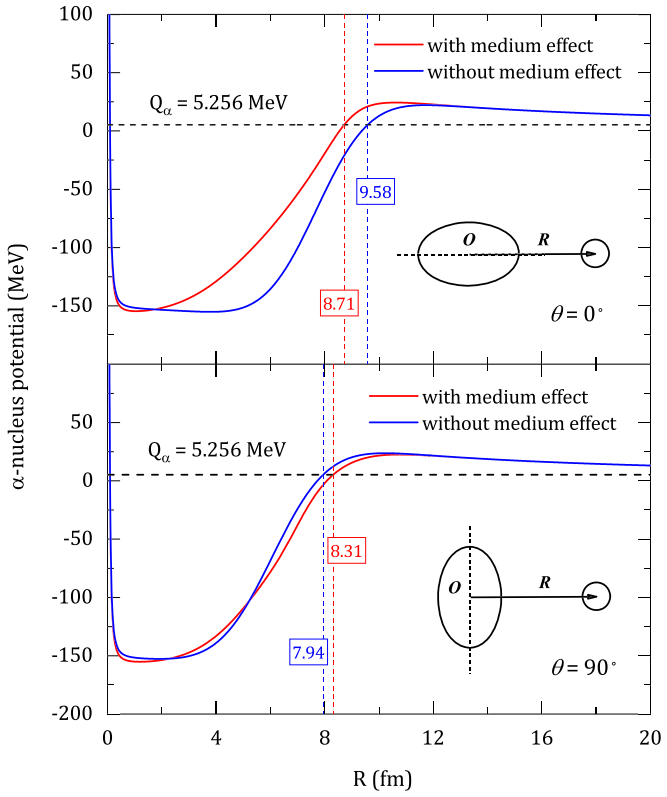

Fig. 6. Impact on the α-nucleus potential due to the nuclear medium effect. The figure shows the total α-nucleus potential at orientation angle $\theta = 0°$ and $\theta = 90°$ for ^{240}Pu (the ^{236}U + α system), of which the daughter nucleus is of well prolate deformation ($\beta_2 = 0.226$, $\beta_4 = 0.108$). The blue and red dash lines with data labels denote the locations of the second classical turning points, which divides the potentials into the internal and the surface regions.

of the corresponding α-nucleus potential. To figure out how the medium effect functions in the α-nucleus interaction, we plot the α-nucleus potentials for the α emitter ^{240}Pu in Fig. 6. Due to the large deformations of its daughter nucleus ^{236}U ($\beta_2 = 0.226$, $\beta_4 = 0.108$), the resulting α-nucleus potential is obviously dependent on the orientation angle θ. In contrast to the spherical cases [18], the medium effect significantly changes the shape of the potential at the surface region. As can be seen that, at $\theta = 0°$ the Coulomb potential barrier is much higher and inside the core region whereas it becomes slightly lower and outside at $\theta = 90°$. Note that such shape variation would be even more evident when the daughter nucleus is of larger deformations. As a direct consequence, the shift of the second classical turning point significantly influences the penetrability and thus, the extracted P_α factor. Comparatively, the effect from the shape variation in the internal region is found to be less evident. It is known that the interior of the potential is mostly associated with the number of the internal nodes of the quasi-bound decaying state, which is chosen according to the Wildermuth rule to account for the Pauli exclusion inside the daughter nucleus. For ^{240}Pu, the change of the internal geometry of the potential contributes to 17% increase in the normalization factor F in Eq. (9), while the penetrability P increases by 65% due to shape variation in the surface region. This indicates the surface transformation from the medium effect is more prominent for α decay, which also holds for the spherical case [18]. Therefore, Fig. 6 is a direct manifestation of the nuclear medium effect in the α-nucleus potential.

4. Summary

In the present study, we propose the dynamic double-folding α-nucleus potential (DDFP) which naturally embodies the nuclear medium effect that the α cluster dynamically changes its size while tunnelling the Coulomb potential barrier. To evaluate the influence due to this medium effect, we perform a systematic calculation of α-decay rates for known even-even α emitters and compare the results with those by the conventional double-folding potential. It is found that the medium effect optimises the surface geometry of the α-nucleus interaction and is highly associated with the nuclear deformations. In consequence, the obtained average deviation between the theoretical and experimental decay rates is about 23% less than before, which indicates a very significant improvement for half-life calculations. The result reveals the important role of the dynamic clustering effect in describing the α-nucleus interaction.

In addition, as an alternative to the microscopic quartetting wavefunction approach [15], the present study presents an semi-classical method to include the nuclear medium effect into the effective α-nucleus interaction. We show the medium effect can directly enter into the potential through the dynamic α-cluster density distribution, thus avoiding the complexity in solving the many-body in-medium equation for the α cluster. However, one should still remember the approximation for the density distribution of the daughter nucleus, where a frozen Fermi distribution is employed. This means the daughter's structural details as well as its correlations with the α cluster is currently absent in DDFP. Therefore, to consider the dynamics of the daughter's density profile is one promising way to improve the present approach. To go beyond the present study, one can further improve the density-dependence in the β function, by using distinguished dependencies on neutron and proton densities, so that the neutron skin (halo) structure at the surface of the daughter nucleus can also be included.

Acknowledgements

Daming Deng and Zhongzhou Ren thank Professor P. Schuck and Professor G. Röpke for the inspiring discussions during the Workshop of Nuclear Cluster Physics (WNCP2018). This work is supported by the National Natural Science Foundation of China (Grant No. 11535004, No. 11761161001, No. 11375086, No. 11120101005, No. 11175085, No. 11235001, No. 11475115), the National Major State Basic Research and Development of China (Grant No. 2016YFE0129300), the Science and Technology Development Fund of Macau (Grant No. 008/2017/AFJ, No. 068/2011/A), and by the Natural Science Foundation of SZU (Grant No. 2019100).

Appendix A. Supplementary material

Supplementary material related to this article can be found online at https://doi.org/10.1016/j.physletb.2019.06.045.

References

[1] D.J. Rowe, Rep. Prog. Phys. 48 (1985) 1419.
[2] W. von Oertzen, Martin Freer, Yoshiko Kannada-En'yo, Phys. Rep. 432 (2006) 43.
[3] Zhongzhou Ren, Bo Zhou, Front. Phys. 13 (2018) 132110.
[4] K. Varga, R.G. Lovas, R.J. Liotta, Phys. Rev. Lett. 69 (1992) 37.
[5] F. Hoyler, P. Mohr, G.S. Staudt, Phys. Rev. C 50 (1994) 2631.
[6] S. Ohkubo, Phys. Rev. Lett. 74 (1995) 2176.
[7] A. Astier, P. Petkov, M.-G. Porquet, D.S. Delion, P. Schuck, Phys. Rev. Lett. 104 (2010) 042701.
[8] K. Auranen, D. Seweryniak, M. Albers, et al., Phys. Rev. Lett. 121 (2018) 182501.
[9] R.G. Lovas, R.J. Liotta, A. Insolia, et al., Phys. Rep. 294 (1998) 265.

[10] P. Schuck, Y. Funaki, H. Horiuchi, et al., Phys. Scr. 91 (2016) 123001.
[11] K. Harada, Prog. Theor. Phys. 26 (1961) 667.
[12] V.G. Soloviev, Phys. Lett. 1 (1962) 202.
[13] I. Tonozuka, A. Arima, Nucl. Phys. A 323 (1979) 45.
[14] D.S. Delion, R.J. Liotta, Phys. Rev. C 87 (2013) 041302.
[15] G. Röpke, P. Schuck, Y. Funaki, et al., Phys. Rev. C 90 (2014) 034304.
[16] Chang Xu, Zhongzhou Ren, G. Röpke, et al., Phys. Rev. C 93 (2016) 011306(R).
[17] Chang Xu, G. Röpke, P. Schuck, et al., Phys. Rev. C 95 (2017) 061306(R).
[18] Daming Deng, Zhongzhou Ren, Phys. Rev. C 96 (2017) 064306.
[19] G.R. Satchler, W.G. Love, Phys. Rep. 55 (1979) 183.
[20] Chang Xu, Zhongzhou Ren, Phys. Rev. C 73 (2006) 041301(R).
[21] D.M. Brink, J.J. Castro, Nucl. Phys. A 216 (1973) 109.
[22] G. Röpke, A. Schnell, P. Schuck, P. Nozières, Phys. Rev. Lett. 80 (1998) 3177.
[23] H. Takemoto, M. Fukushima, S. Chiba, et al., Phys. Rev. C 69 (2004) 035802.
[24] T. Sogo, G. Ropke, P. Schuck, Phys. Rev. C 81 (2010) 064310.
[25] M. Girod, P. Schuck, Phys. Rev. Lett. 111 (2013) 132503.
[26] D.T. Khoa, G.R. Satchler, W. von Oertzen, Phys. Rev. C 56 (1997) 954.
[27] S.A. Gurvitz, G. Kalbermann, Phys. Rev. Lett. 59 (1987) 262.
[28] P.E. Hodgson, E. Běták, Phys. Rep. 374 (2003) 1.
[29] Daming Deng, Zhongzhou Ren, Phys. Rev. C 93 (2016) 044326
.